Psychophysiology, 31 (1994), 44–61. Cambridge University Press. Printed in the USA.

Autonomic space and psychophysiological response

GARY G. BERNTSON, JOHN T. CACIOPPO, KAREN S. QUIGLEY,
AND VINCENT T. FABRO
Department of Psychology, Ohio State University, Columbus

Abstract

Contemporary findings reveal that autonomic control of dually innervated target organs cannot adequately be viewed as a continuum extending from parasympathetic to sympathetic dominance. Rather, a two-dimensional autonomic space, bounded by sympathetic and parasympathetic axes, is the minimal representation necessary to characterize the multiple modes of autonomic control. We have previously considered the theoretical implications of this view and have developed quantitative conceptual models of the formal properties of autonomic space and its translation into target organ effects. In the present paper, we further develop this perspective by an empirical instantiation of the quantitative autonomic space model for the control of cardiac chronotropy in the rat. We show that this model (a) provides a more comprehensive characterization of cardiac response than simple measures of end-organ state, (b) permits a parsing of the multiple transformations underlying psychophysiological responses, (c) illuminates and subsumes psychophysiological principles, such as the Law of Initial Values, (d) reveals an interpretive advantage of expressing cardiac chronotropy in heart period rather than heart rate, and (e) has fundamental implications for the direction and interpretation of a broad range of psychophysiological studies.

Descriptors: Autonomic nervous system, Autonomic space, Autonomic control, Autonomic modes, Heart period, Chronotropic state, Parasympathetic, Sympathetic

The sympathetic and parasympathetic branches of the autonomic nervous system (ANS) have traditionally been viewed as subject to reciprocal central control, with increasing activity of one branch associated with decreasing activity of the other. This doctrine of autonomic reciprocity offered an autonomic parallel to Sherrington's (1906) influential concept of reciprocal innervation within the somatic nervous system and provided a simple theoretical vantage for conceptions of the nature of autonomic control. Although the reciprocal model represents one common mode of ANS regulation, exceptions to this pattern of autonomic control have been recognized historically. Early work of Gellhorn and colleagues suggested that coactivation of both vagal and sympathetic divisions of the ANS could be seen under some conditions (Gellhorn, Cortell, & Feldman, 1941). Even organ selective patterns of autonomic coactivation were implicit in Cannon's (1939) metaphor, in which the parasympathetic system was likened to the keys of a piano and the sympathetic division to its pedals. These early perspectives presaged contemporary views, which emphasize the flexibility with which central mechanisms can modulate autonomic outflows. It is now clear that autonomic coactivation, as revealed by direct neurophysiological recordings and psychophysiological measures, can be triggered by basic cardiovascular reflexes as well as by behavioral states or processes (Berntson, Cacioppo, & Quigley, 1991; Fukuda, Sato, Suzuki, & Trzebski, 1989; Iwata & LeDoux, 1988; Koizumi, Kollai, & Terui, 1986; Koizumi, Terui, & Kollai, 1983; Obrist, Wood, & Perez-Reyes, 1965; Quigley & Berntson, 1990). Activity in the two ANS divisions may vary reciprocally, coactively, or independently (see Berntson et al., 1991).

The multiple modes of autonomic control have substantial implications for psychophysiological concepts, the selection of response measures, and the design and interpretation of psychophysiological studies. We have recently proposed a general quantitative model of autonomic control and consequence, which subsumes the doctrine of autonomic reciprocity within a broader conception of the multiple modes of autonomic control (Berntson et al., 1991). In the present paper, we (a) give a brief overview of this conceptual model of autonomic control, (b) expand on this conception and provide a quantitative instantiation of this general model for autonomic control of cardiac chronotropy in the rat, (c) illustrate the utility of this model in specifying basal and dynamic patterns of autonomic control in behavioral contexts, and (d) consider the extension of this model to humans and its implications for psychophysiology.

A Quantitative Model of Autonomic Space

The essence of the traditional doctrine of autonomic reciprocity is an autonomic vector or continuum, which extends from sympathetic activation at one end to parasympathetic activation at the other extreme. According to this model, the state of autonomic control at any given time is characterized by a point on this continuum. An autonomic continuum, however, fails to adequately represent instances of coactivation or coinhibition

Address reprint requests to: Gary G. Berntson, 48 Townshend Hall, Ohio State University, Columbus, OH 43212.

Table 1. *Modes of Autonomic Control*

	Parasympathetic response		
Sympathetic response	Increase	No change	Decrease
Increase	coactivation	uncoupled sympathetic activation	reciprocal sympathetic activation
No change	uncoupled parasympathetic activation	baseline	uncoupled parasympathetic withdrawal
Decrease	reciprocal parasympathetic activation	uncoupled sympathetic withdrawal	coinhibition

of the sympathetic and parasympathetic branches or independent changes in a single autonomic division. We outline below a more comprehensive two-dimensional model of autonomic space, which subsumes the doctrine of autonomic reciprocity and embodies the alternative modes of control.

Modes of Autonomic Control

The potential patterns of autonomic control over dually innervated target organs are outlined in Table 1, which depicts all classes of increased, decreased, or unaltered activity in the two ANS divisions. The nine cells of Table 1 can be further grouped into three major categories: (a) coupled reciprocal modes, in which activities of the two divisions are negatively correlated, (b) coupled nonreciprocal modes, in which activities are positively correlated, and (c) uncoupled modes, in which activity changes are uncorrelated. The classical reciprocal patterns, in which activities of the two divisions are negatively correlated, are represented by the cells in the upper right (reciprocal sympathetic mode) and the lower left (reciprocal parasympathetic mode). Coupled responses in which the activities of the two divisions are positively correlated are represented by the cells in the upper left (coactivation) and lower right (coinhibition). The remaining cells (except baseline) depict autonomic responses in one ANS division that are uncorrelated with changes in the other (uncoupled sympathetic and uncoupled parasympathetic modes).

The modes of autonomic control have distinct functional properties (Berntson et al., 1991). Given opposing influences of the autonomic divisions, reciprocal changes in the two autonomic divisions yield mutually synergistic effects on the target organ.[1] Hence, the reciprocal mode exhibits the widest dynamic range of control and yields the greatest target organ reactivity. Moreover, because the changes in both divisions produce similar directional responses in the target organ, reciprocal modes yield a high degree of directional stability in the organ response. In contrast, nonreciprocal modes of coactivation and coinhibition tend to minimize functional responses of the target organ, because changes in the two autonomic branches yield opposing effects. Thus, both the dynamic range and the reactivity are reduced. Moreover, nonreciprocal modes have a fundamental instability in response direction that depends on which autonomic division predominates. The uncoupled modes have features intermediate to those of the reciprocal and nonreciprocal modes of control.

[1]These functional properties apply for dually innervated organs that receive antagonistic innervations from the two ANS divisions. With synergistic actions, the properties of reciprocal and nonreciprocal modes would be reversed.

Two-Dimensional Autonomic Space

The modes of Table 1 and the intermediate forms exhaust the potential patterns of autonomic control at any given moment. Each of the modes of Table 1 has been documented in both physiological and behavioral studies (see Berntson et al., 1991). In view of these findings, autonomic control cannot be viewed as lying along a single vector or continuum extending from parasympathetic to sympathetic dominance. Rather, a two-dimensional autonomic plane, as illustrated in Figure 1, is the minimal representation required to capture the multiple modes of autonomic control. This conception of autonomic space subsumes the doctrine of reciprocity along the reciprocal diagonal, which extends from sympathetic to parasympathetic dominance. The model also incorporates nonreciprocal modes, in which activities of the two autonomic branches are positively correlated, as vectors along or parallel to the diagonal of coactivity. This two-

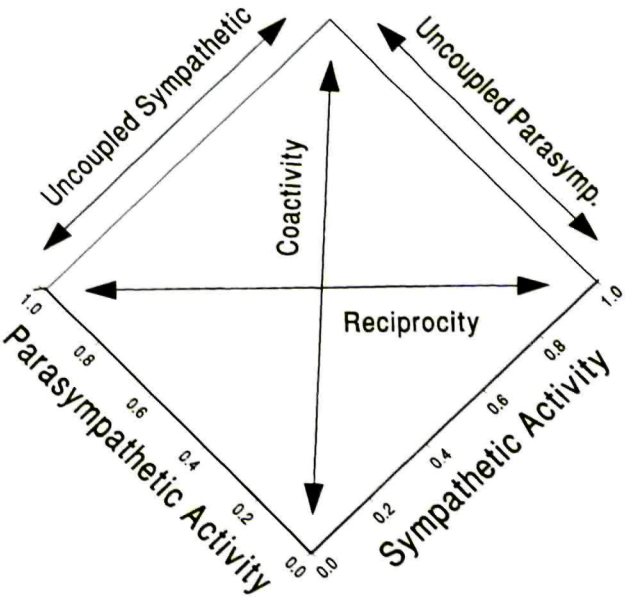

Figure 1. Two-dimensional representation of autonomic space. Axes units are expressed as a proportional activation of the sympathetic and parasympathetic branches. On the diagonal of reciprocity, increased activity in one autonomic division is associated with decreases in the other. On the diagonal of coactivity, activities in the autonomic branches concurrently increase (coactivation) or decrease (coinhibition). The arrows along the axes depict uncoupled changes in the single ANS divisions. These arrows, and vectors parallel to them, illustrate the major modes of autonomic control.

dimensional autonomic space represents uncoupled modes as vectors along or parallel to the marginal axes.

Autonomic Space and Target-Organ Effects

Psychophysiological relationships entail two major classes of transformations: (a) from psychophysiological antecedents to autonomic outflows and (b) from autonomic outflows to functional effects on target organs. An inherent confound therefore exists as to the form and locus of psychophysiological relationships, because transformations at one stage can obscure or confound other transformational stages. By quantifying autonomic space and its manifestations at end organs, variance in psychophysiological data associated with the second of these transforms can be specified. Elimination of this source of variance may clarify or reveal psychophysiological relationships that would otherwise remain obscure.

The two-dimensional autonomic plane depicted in Figure 1 represents all possible levels of autonomic outflow to the target organ. Each point within this autonomic plane specifies a unique combination of sympathetic and parasympathetic activities, which will manifest in some physiological effect on the target organ. The development of a comprehensive model of autonomic control requires the specification of the functions relating patterns of autonomic outflow to physiological manifestations at the end organ. A general equation expresses this transformation:

$$f_{ij} = \beta + C_s \cdot S_i + C_p \cdot P_j + I_{ij} + \epsilon, \qquad (1)$$

where f_{ij} is the functional state of the target organ for any i (sympathetic) and j (parasympathetic) locus in autonomic space, β is the basal functional state in the absence of autonomic input, S_i and P_j are the independent activities of the sympathetic and parasympathetic innervations at point ij, and C_s and C_p are coupling coefficients, which reflect the relative functional impact of sympathetic and parasympathetic activities on the target organ. For illustrative purposes, potential interactions among the ANS divisions are expressed in the general term I_{ij}, which can be expanded into polynomial components ($S_i \cdot P_j$, $S_i^2 \cdot P_j$, $S_i \cdot P_j^2$, $S_i^2 \cdot P_j^2$). ϵ is an error term that includes, among other things, local (nonneural) hormonal, thermal, and metabolic effects.

Equation 1 represents a general form of the quantitative model of Levy and Zieske (1969) for the autonomic control of the heart. The terms of this equation reflect the three principles of autonomic control outlined by Berntson et al. (1991). The principle of innervation states that target organs can be either singly or dually innervated by the autonomic branches. For dually innervated organs, both coupling coefficients are nonzero, whereas for singly innervated organs, one coefficient is set to zero. The principle of conjoint action maintains that the two autonomic divisions may have either opposing or synergistic actions on dually innervated organs. This principle is manifest in the signs of the coefficients C_s and C_p, which are equivalent for concordant actions and opposite for opponent actions. The principle of multiple modes stipulates that the two autonomic branches may vary independently. This principle is reflected in the separate activation functions S_i and P_j, where i and j may vary reciprocally, nonreciprocally, or independently.

Equation 1 provides an estimate of the functional state of a target organ for any locus in autonomic space. This target organ state can be described by an effector surface overlying the two-dimensional autonomic plane.

Empirical Instantiation of Autonomic Space in the Rat

Equation 1 and its representation of the autonomic effector surface have been useful in the exploration and quantitative modeling of general principles of autonomic control (Berntson et al., 1991). Specific psychophysiological applications would further benefit from an empirical implementation of this general model for a given target organ in humans. For initial model development, however, the greater control and experimental flexibility with animals offer considerable advantages. We present an empirical instantiation of this model for the chronotropic control of the heart in rats. The rat is increasingly employed in cardiovascular research, and a large body of behavioral and physiological literature exists on this species.

The instantiation of a quantitative model of autonomic space requires specification of four sets of parameters that define the terms of Equation 1: (a) the intrinsic heart rate (β) in the absence of autonomic control; (b) the dynamic ranges of sympathetic and parasympathetic chronotropic control, which define the values of the coefficients C_s and C_p; (c) the effector-transform functions of the marginal sympathetic and parasympathetic axes (S_i and P_j); and (d) the potential interactions among the branches, which allow specification of the interaction term (I_{ij}). These parameters permit the construction of an effector surface for chronotropic control of the heart in a given species.

Intrinsic Heart Period

The intrinsic heart period (β), or zero point of autonomic control, can be indexed by dual pharmacological blockade of the autonomic branches or by surgical denervation of the autonomic control of the heart (Randall, Kaye, Randall, Brady, & Martin, 1976, Randall, Kaye, Thomas, & Barber, 1980). For the Sprague-Dawley rat, reported basal heart period under complete dual blockade has been quite consistent, ranging from 158 ms (Head & McCarty, 1987) to 161 ms (Corre, Cho, & Barnard, 1976) or to 166 ms from our laboratory.[2] The average of these values (162 ms, corresponding to a heart rate of 370 bpm) provides an estimate of the chronotropic state of the heart at the (0, 0) intersection of Figure 1. This value compares closely with estimates from our laboratory derived from the results of single blockades (160 ms)[3] and to estimates for rats of the Wistar (166 ms; Lin, 1974) and Wistar-Kyoto (169 ms; Murphy, Sloan, & Myers, 1991) strains.

[2] We express chronotropic state in terms of heart period rather than heart rate. Heart period constitutes a linear scale, whereas heart rate represents a nonlinear transform of this scale. The linearity of the heart period scale confers considerable advantages for the development of quantitative models of chronotropic control.

[3] Lin and Horvath (1972) described a subtractive method for deriving intrinsic heart period from the results of single blockades of the autonomic divisions. Unlike dual blockade, this method is subject to potential confound from indirect reflex effects of blockade of one division on the activity of the unblocked division. This method, however, generally yields results that are concordant with those of dual blockade.

Dynamic Ranges of the Autonomic Branches

The weighting coefficients (C_s and C_p) represent the dynamic ranges of the autonomic divisions. With the units of the autonomic axes (S_i and P_j) expressed as a proportional activation (from 0 to 1), these coefficients represent the absolute ranges of sympathetic and parasympathetic chronotropic control (in milliseconds). These coefficients can be estimated given a knowledge of (a) the intrinsic heart period, (b) the heart period under maximal sympathetic control (HPs_{max}), and (c) the heart period under maximal parasympathetic control (HPp_{max}). In the absence of parasympathetic control, the sympathetic coefficient is defined as

$$C_s = HPs_{max} - \beta. \tag{2a}$$

Similarly, in the absence of sympathetic control, the parasympathetic coefficient is

$$C_p = HPp_{max} - \beta. \tag{2b}$$

Maximum sympathetic control. An estimate of HPs_{max} can be derived from heart period under exercise. Exercise to exhaustion yields maximal sympathetic activation and complete parasympathetic withdrawal of the chronotropic control of the heart (Bolter & Atkinson, 1988a; Corre, Cho, & Barnard, 1976; Ekblom, Kilbom, & Soltysiak, 1973). For example, administration of a beta-adrenergic agonist (isoproterenol) yields no further decrease in heart period after maximal exercise in the rat (Bolter & Atkinson, 1988b), and parasympathetic blockade has no effect on heart period under these conditions (Corre et al., 1976; Ekblom et al., 1973). These findings indicate a maximal endogenous sympathetic control of the heart and a nonsignificant residual parasympathetic influence under extreme exercise.

Although the shortest heart period (maximal heart rate) during exercise in rats varies somewhat with weight, sex, and strain, these variations are minimal for adult animals. Reported values generally range from 100 to 110 ms (Bolter & Atkinson, 1988a; Corre et al., 1976; Sonne & Galbo, 1980), yielding an estimated maximal exercise heart period of 105 ± 5 ms (571 bpm) for the rat. A component of the heart period effect of exercise, however, is attributable to direct thermal effects on the cardiac pacemaker, which have been quantitatively defined for the rat (Bolter & Atkinson, 1988b). When the formula of Bolter and Atkinson is employed to remove direct effects of temperature, HPs_{max} for the Sprague-Dawley rat is ≈120 ms (corresponding to a heart rate of 500 bpm).

Converging evidence on this value comes from two independent lines of evidence. Bolter and Atkinson (1988a) employed the beta-adrenergic agonist isoproterenol, both in vivo and in vitro, to estimate the maximal sympathetic effect on cardiac chronotropy in the rat. The minimum heart periods obtainable with isoproterenol were 122 ms in vivo and 121 ms in vitro. These values correspond closely to the 120 ms derived from exercise data. A second line of converging information comes from a study of the baroreflex in the rat (Head & McCarty, 1987). Bolus infusions of nitroprusside were employed to decrease blood pressure and yield a baroreflex activation of sympathetic outflow and inhibition of vagal control of the heart. With maximal baroreflex activation, administration of atropine failed to significantly affect heart period, indicating a complete withdrawal of vagal control at the extremes of hypotension. Under these conditions, the baroreflex yielded an asymptotic sympathetic activation at a heart period of 119 ms. This index of maximal sympathetic control, which would be largely unconfounded by thermal effects, is highly comparable to the estimated 120 ms derived from exercise data.

Based on these converging lines of evidence, the mean estimate of HPs_{max} for the rat is ≈120 ms, which represents less than a 2% disparity from the values of the three independent estimates derived above. This estimate reflects both the direct sympathetic neural innervation of the heart and the indirect sympathoadrenal component, both of which reflect central sympathetic outflows.[4]

Maximum parasympathetic control. An estimate of HPp_{max} is also available for the rat. Among the most potent influences on vagal control of the heart is the dive reflex. This is a life-preserving response to submersion, triggered by trigeminal afferents and chemoreceptors (Daly, 1984). The dive reflex entails a redistribution of blood to the central core, coupled with a massive vagal outflow. Although this reflex is most fully developed in diving species, it is also striking in humans and other terrestrial mammals and probably accounts for the remarkable survival of children after prolonged submersion. In rats, the diving reflex results in a striking increase in vagal outflow and a virtually complete withdrawal of sympathetic cardiac tone. Diving bradycardia is largely eliminated by parasympathetic blockade but is not attenuated by sympathetic blockade or adrenergic depletion (Lin, 1974). Two controlled studies of the dive reflex in unanesthetized rats revealed a rapid increase in heart period to 403 ms (Huang & Peng, 1976) and 419 ms (Lin, 1974), yielding a mean estimate for HPp_{max} of ≈411 ms.[5]

These end-point estimates of HPs_{max} and HPp_{max} provide anchors for the normal extremes of autonomic control of cardiac chronotropy. Ideally, however, additional convergent evidence for the estimate of HPp_{max} from alternative measures would be desirable. Moreover, further information is necessary to define the shapes of the marginal functions of the autonomic axes.

Autonomic Transfer Functions: Autonomic Outflows and Effector Response

Considerable evidence indicates that the axes functions (S_i and P_j) of autonomic space show an essentially linear relationship with cardiac chronotropy (expressed in heart period) over their full dynamic range. The most definitive lines of evidence come from direct neural stimulation and recording studies of the cardiac nerves. Early stimulation studies (e.g., Carlsten, Folkow, & Hamberger, 1957; Rosenbleuth, 1932) generally reported a

[4]Studies in both humans and dogs show that total cardiac denervation or heart transplant largely eliminate dramatic, short-latency cardiac responses in behavioral contexts (Randall, Kaye, Randall, Brady, & Martin, 1976; Sloan, Shapiro, & Gorman, 1990). Adrenomedullary catecholamines, however, could sometimes manifest in delayed and greatly attenuated responses. Neural and adrenal components of sympathetic control could be parsed in future refinements of the present model by adrenalectomy or the use of selective catecholamine receptor antagonists and blockers of catecholamine release from sympathetic nerve terminals (see Tucker & Domino, 1988).

[5]Because anesthesia or severe anoxia can seriously confound the estimate of parasympathetic control, we excluded studies that employed anesthetized animals or prolonged dive durations (>30 s).

hyperbolic relationship between vagal stimulation frequency and heart rate. When expressed as heart period, however, these relationships become linear. More recent studies have confirmed the approximately linear relationship between vagal stimulation frequency and heart period in humans, dogs, cats, and rabbits (Carlson et al., 1992; Dexter, Levy, & Rudy, 1989; Ford & McWilliam, 1986; Furukawa, Wallick, Carlson, & Martin, 1990; Parker, Celler, Potter, & McCloskey, 1984; Stramba-Badiale et al., 1991; Versprille & Wise, 1971). Moreover, a relatively linear function has been reported for the relationship between heart period and endogenous vagal activity (Katona, Poitras, Barnett, & Terry, 1970; Koizumi, Terui, & Kollai, 1985). Although linear relations in biological systems are rare, the quantitative biophysical model of Dexter et al. (1989) reveals that this linearity arises as a result of two nonlinear processes. Specifically, the model maintains that accumulation of acetylcholine (ACH) at cardiac effector synapses is a negatively accelerating function of vagal activity, whereas the effect of ACH on cardiac chronotropy is a positively accelerating function of concentration. The result of these two nonlinear processes is the observed linear relationship between vagal frequency and heart period.

We have recently confirmed the linearity between vagal frequency and heart period in the rat through direct stimulation of the vagus nerve (Berntson et al., 1992). Regression functions of heart period on stimulation frequency revealed that 93–97% of the variance in heart period could be explained by the linear component. Figure 2a shows the results of vagal stimulation in a representative animal. We have also found a similar linearity with direct stimulation of the central vagal source nuclei (nucleus ambiguus) in the rat (Figure 2b).

In addition to defining the shape of the vagal marginal function, this stimulation study also provides converging information on the value of HPp_{max}, as identified from the literature on the dive reflex. At maximal frequencies, vagal stimulation in the rat consistently yielded chronotropic effects that exceeded normal physiological levels, resulting in sinus block or other severe arrhythmias (Berntson et al., 1992). This end-point value was highly consistent across animals and provides an additional estimate of the maximal vagal control of the heart. This maximal heart period value averaged 401 ms, which approximates that identified from the dive reflex (411 ms). The average of these two indices of maximal vagal control yields an estimated HPp_{max} of $\approx$406 ms, which is within 2% of the independent estimates derived from the literature on the dive reflex and from neural stimulation.

Although the parasympathetic innervation can exert extreme chronotropic actions that exceed normal physiological limits, chronotropic actions of the sympathetic system are more limited and generally show a clear asymptotic maximum. However, the frequency of sympathetic stimulation shows an approximately linear relationship with heart period, up to asymptotic levels. As with vagal stimulation, this linearity between stimu-

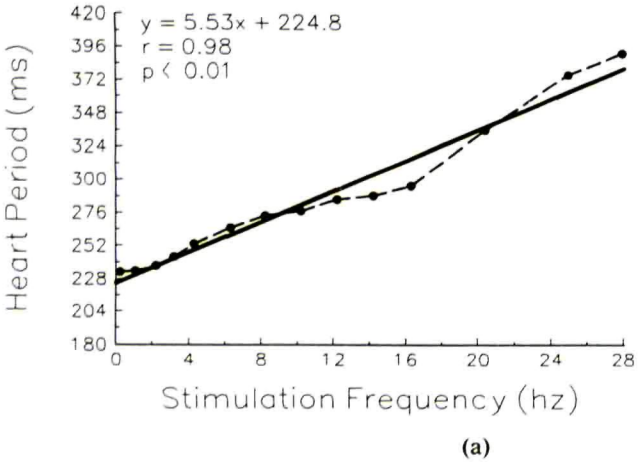

(a)

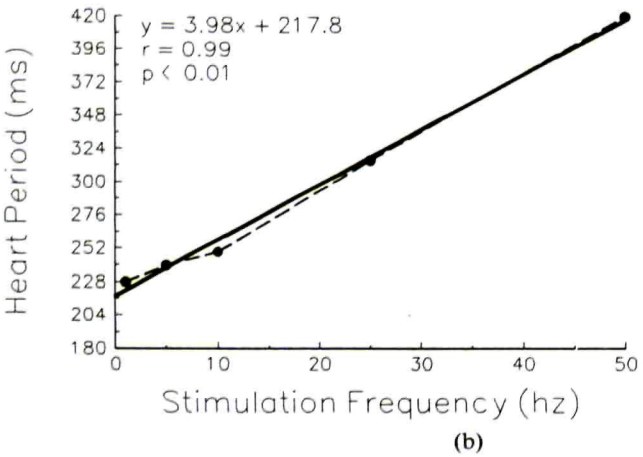

(b)

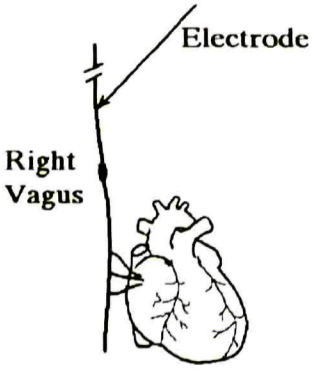

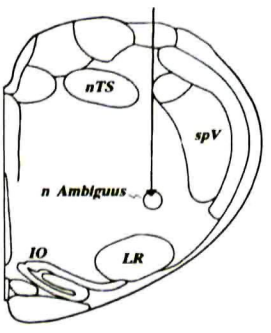

Figure 2. Chronotropic effects of vagal stimulation. (a) Effects of direct electrical stimulation of the decentralized right vagus nerve, as a function of stimulation frequency in a representative animal. Sympathetic cardiac effects were blocked by atenolol (5 mg/kg). [Data derived from Berntson, Quigley, Fabro, & Cacioppo, 1992.] (b) Effects of direct electrical stimulation of the vagal source nuclei, as a function of stimulation frequency under comparable conditions. The dashed lines depict the obtained data, and the solid lines illustrate the linear regression function. [Data are from unpublished studies on central stimulation following the same general protocols as Berntson, Quigley, Fabro, & Cacioppo, 1992.]

lus frequency and heart period appears to be species general (Berger, Saul, & Cohen, 1989; Kerin, Louridas, Edelstein, & Levy, 1983; Levy & Zieske, 1969). Similarly, a linear function has been reported for the relationship between heart period and endogenous sympathetic activity over relatively wide variations in heart period (Koizumi et al., 1985). These studies uniformly indicate that the shape of the marginal functions for autonomic space has an essentially linear relationship to cardiac chronotropy expressed in heart period.

The linearity between autonomic outflows and heart period confers both pragmatic and theoretical advantage to the specification of cardiac chronotropy in heart period rather than heart rate. First, units of time, rather than transformed units of rate, have a more natural relationship to the temporally dependent ionic processes of sinoatrial pacemaker cells (Dexter et al., 1989). Time units are necessary for analysis of cardiac cycle effects or other within-beat processes. Second, because period is a linear scale, a given unit change in heart period is equivalent regardless of the basal starting point, an identity that does not hold for rate measures. Third, because heart period is linearly related to autonomic activities, a given millisecond change in heart period represents an equivalent change in autonomic outflow independent of baseline.

A Quantitative Model of Chronotropic Control in the Rat

Given the estimate of β (162 ms) and the end points of autonomic control ($HPs_{max} = 120$ ms; $HPp_{max} = 406$ ms) as defined above, the values of the coefficients can be derived from Equations 2a and 2b. Specifically, the sympathetic coefficient is 120 − 162 ms = −42 ms, and the parasympathetic coefficient is 406 − 162 ms = 244 ms. Inserting these values into Equation 1 gives

$$f_{ij} = 162 - 42S_i + 244P_j + I_{ij} + \epsilon. \quad (3)$$

The cardiac (chronotropic) effector surface. In the absence of interactions, Equation 3 yields a cardiac effector surface that represents the heart period for all points on the autonomic plane (i.e., all possible combinations of sympathetic and parasympathetic activities). The autonomic plane and effector surface illustrated in Figure 3 exhaustively represent all loci within autonomic space and the chronotropic state of the heart for each locus within this space. Each of the autonomic axes range from 0 to 1, reflecting the proportional activation in the corresponding autonomic division. For the illustration, the lengths of the axes are scaled relative to the overall dynamic range of sympathetic and parasympathetic chronotropic control (i.e., by the magnitude of the coefficients C_s and C_p). This normalizes directional displacements of a given distance on the effector surface to equivalent heart period changes.

Isoeffector contours. On the surface depicted in Figure 3, a given chronotropic state of the heart is ambiguous with regard to its autonomic origins. This is evident in the isoeffector contour lines projected onto the autonomic plane of this figure. These contours illustrate the multiple loci on the autonomic plane that yield an equivalent psychophysiological state of the target organ. This many-to-one mapping underscores the indeterminism when inferring changes in autonomic activities or behavioral processes based solely on changes in the functional state of dually innervated organs. Because identical psychophysiological outcomes may arise from different autonomic loci, information beyond a simple measure of target state may be necessary to determine autonomic origins of a psychophysiological response. The autonomic space model, however, makes it possible to uniquely specify autonomic responses as a function of movements along the two autonomic axes.

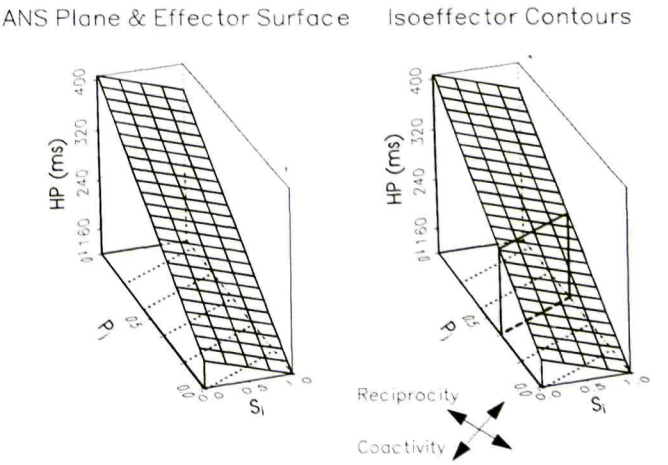

Figure 3. Two-dimensional autonomic plane and its associated effector surface. The effector surface represents the chronotropic state of the target-organ for all loci within autonomic space, as derived from Equation 3. The axes dimensions are in proportional units of activation. The length of the axes are scaled in proportion to the dynamic range of the autonomic branches so that a given distance along on either axis corresponds to an equivalent heart period change. The dotted lines on the autonomic plane are isoeffector contours, which illustrate loci with equivalent chronotropic effects. The right panel illustrates the translation of one of these isoeffector contours into equivalent chronotropic states on the autonomic surface. The arrows indicate the directional movement vectors associated with reciprocal and coactive modes of autonomic control.

Phasic reactivity as movements within autonomic space. The cardiac effector surface of Figure 3 represents the chronotropic state of the heart associated with all possible loci on the autonomic plane. Hence, knowledge of the location in autonomic space can define the basal chronotropic state of the heart. Moreover, phasic movements within autonomic space translate into a response trajectory across the effector surface. Any change in the location on the autonomic plane would necessarily result in a corresponding movement on the effector surface. Given the existence of isoeffector contours, however, this change may or may not manifest in an alteration of the psychophysiological state of the organ. Consequently, time-varying locations in autonomic space provide an unambiguous account of both the autonomic origins and the temporal dynamics of chronotropic response, even for movements along isoeffector contours that do not manifest in heart period changes.

The effector surface and the modes of control. The modes of autonomic control described in Table 1 can be depicted as directional movements on the effector surface. Reciprocal modes of control are manifested by translations on the effector surface along or parallel to the reciprocal diagonal of autonomic space (left to right axes intersections). In contrast,

autonomic coactivation or coinhibition is reflected by surface translations along or parallel to the diagonal of coactivity (front to back axes intersections). Uncoupled changes in the autonomic divisions manifest in surface translations parallel to the autonomic axes.

The features of the effector surface topography (Figure 3) also illustrate the general properties of the modes of autonomic control. Because reciprocal changes in the two autonomic branches exert mutually supportive effects on the target organ, the reciprocal mode of control yields the highest slope (surface gradient) and the widest dynamic range. In contrast, coactive changes in the two autonomic divisions yield opposing actions on the target organ. Consequently, this mode is associated with a lower slope and a lower dynamic range, as indicated by the coactive diagonal of Figure 3.

Psychophysiological Mapping: Autonomic Space and Effector Surface

The autonomic plane and overlying effector surface provide an important means of mapping psychophysiological responses. To accomplish such mapping, responses must be specified along the two autonomic axes. One approach to estimating the responses along the sympathetic and parasympathetic axes is selective pharmacological blockade of the two autonomic branches, which reveals the independent action of the unblocked division (Berntson et al., 1991; Stemmler, Grossman, Schmid, & Foerster, 1991; Tucker & Domino, 1988).[6]

Orienting and Defensive Reactions

An example of such a mapping is presented in Figures 4 and 5, which illustrate the time-dependent response of rats to a nonsignal acoustic stimulus of two intensities (60 and 80 dB). Consistent with the distinction between orienting and defensive responses, the high-intensity stimulus evoked notable tachycardia or decreased heart period, whereas the low-intensity stimulus resulted in a predominant bradycardia or increased heart period. The autonomic bases of these cardiac responses were investigated (Quigley & Berntson, 1990) by the administration of a parasympathetic antagonist (scopolamine methyl nitrate; 0.1 mg/kg) and a sympathetic beta-1 adrenergic antagonist (atenolol; 5 mg/kg).

Figure 4 illustrates the cardiac response time functions to the two stimuli in the unblocked control condition and after separate blockades of the parasympathetic and sympathetic branches. Pharmacological blockade revealed characteristic features of autonomic coactivation in response to the low-intensity stimulus. The deceleratory response to this stimulus was eliminated by parasympathetic blockade, indicating that this bradycardia arose from a transient increase in parasympathetic control of the heart. Scopolamine not only eliminated the stimulus-induced bradycardia but unmasked a notable cardioacceleratory response to the low-intensity stimulus. The acceleratory response apparent under parasympathetic blockade probably reflected a concurrent sympathetic activation, which is normally obscured by the more potent vagal response. Consistent with this interpretation, sympathetic blockade yielded an increase in the magnitude of the stimulus-induced bradycardia. These results suggest that the low-intensity stimulus induced a coactivation of the two autonomic branches, which mutually opposed or dampened the cardiac manifestations of the other division. Selective blockades, however, were able to reveal the independent activities of the two autonomic divisions.

In contrast to this pattern of autonomic coactivation, the defensive-like response to the high intensity stimulus entailed a more complex temporal pattern consisting of an initial uncoupled sympathetic activation, later accompanied by a moderate reciprocal parasympathetic withdrawal. The acceleratory response to the high-intensity stimulus was dramatically attenuated by sympathetic blockade but was only minimally affected by parasympathetic blockade. Based on the responses obtained under parasympathetic blockade, both the high- and low-intensity stimuli yielded approximately equivalent sympathetic activation throughout the poststimulus period. The primary difference between the responses to the two stimuli appeared to be in the parasympathetic contribution, which increased to the low-intensity stimulus, and decreased to the high-intensity stimulus (see Figure 4).

The expected chronotropic consequences of these autonomic responses were derived by Equation 3, based on independent activities of the autonomic divisions under selective blockade. For these derivations, the interaction term was considered to be null. The chronotropic responses observed in the unblocked conditions are replotted, along with the predicted response templates, in the right panels of Figure 4. Any bias in the estimates of the independent activities of the autonomic branches, arising for example from incomplete blockades or from indirect effects of the pharmacological agents, would yield a predicted response template that deviated from that observed in the unblocked condition. The predicted and observed heart period functions of Figure 4 showed a relatively close correspondence, suggesting that the blockers provided accurate estimates of the activities of the autonomic branches. This correspondence is especially notable because the control and blockade data were obtained in separate (counterbalanced) sessions on separate days. The results further indicate that Equation 3 may yield a relatively good approximation of the unblocked response, even in the absence of an interaction term.

[6] Interpretation of the results of autonomic blockade is discussed in Berntson, Cacioppo, and Quigley (1991) and Stemmler, Grossman, Schmid, and Foerster (1991). The validity of inferences derived from autonomic blockades is dependent on two assumptions: (a) that the pharmacological blockades are relatively complete and (b) that blockade of one division does not indirectly alter the activity of the unblocked division. Incomplete blockades can underestimate the independent activities of the autonomic branches, because residual influences of the partially blocked division continue to contaminate heart period responses. Ideally, studies employing pharmacological antagonists should include a dual blockade condition to confirm the effectiveness of the autonomic blockades. A second source of confound can arise from potential indirect effects of autonomic blockade, including reflex adjustments, which alter the activity of the unblocked division. This problem is generally less important for heart period, because cardiac chronotropy is not directly monitored and regulated physiologically. Fortunately, it is possible to explicitly test for such confounds and for interactions among the autonomic branches that could confound analyses. Equation 3 permits the derivation of an expected heart period response template, based on the independent estimates of the activities of the autonomic branches. Any bias in the estimates of these autonomic activities, derived from blockade conditions, would yield an expected response template that deviates from the response observed in the unblocked condition. The absence of appreciable distortions of chronotropic measures from selective autonomic blockade is indicated by the close agreement between the observed unblocked cardiac responses and those predicted by Equation 3 as derived from selective blockades. Stemmler et al. (1991) offered quantitative strategies for dealing with these confounds when discrepancies are apparent.

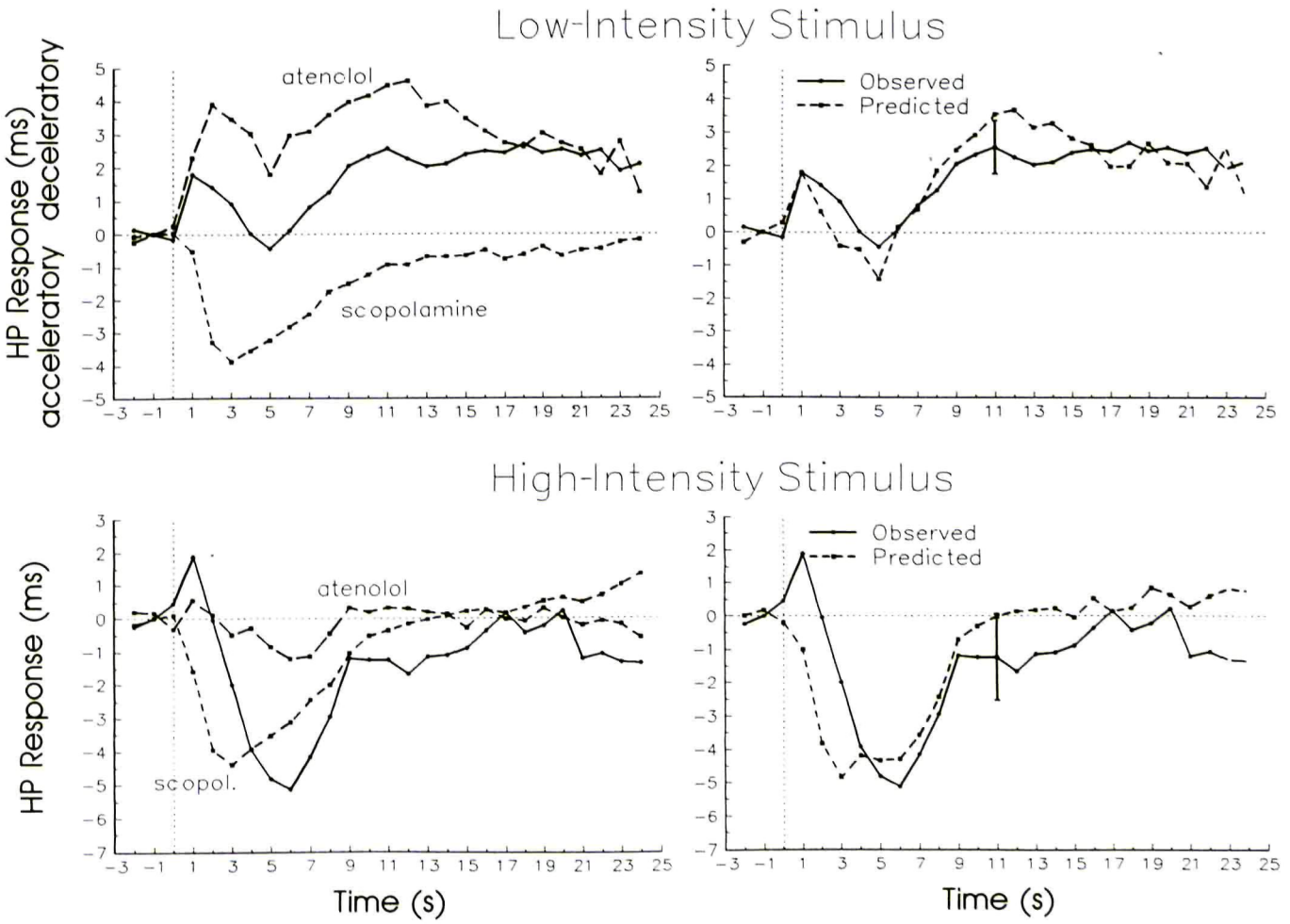

Figure 4. Mean cardiac responses of rats (*N*s = 12–14) to a nonsignal acoustic stimulus of low intensity (60 dB) and high intensity (80 dB). Left panels illustrate the heart period responses in the unblocked condition (solid lines) and after sympathetic (atenolol, 5 mg/kg) or parasympathetic (scopolamine methyl nitrate, 0.1 mg/kg) blockade. Right panels illustrate the observed response in the unblocked condition and the predicted responses derived from Equation 3, based on the independent responses of the autonomic branches under selective blockades. Error bars depict illustrative standard errors for the unblocked response. [Redrawn with permission from Quigley & Berntson, 1990.]

The data of Figure 4 are replotted on the effector surface in Figure 5. The most striking feature of this representation is the relatively limited response range on the autonomic effector surface. Consequently, the relevant segment of the effector surface is expanded in Figure 5 for illustration. The expanded inserts depict the temporally unfolding cardiac response as movements along the two autonomic axes. The data points in the inserts represent the momentary autonomic locus over successive seconds, beginning at the baseline locus at the (0, 0) intersection. For illustration, the axes units are expressed in millisecond change in heart period (i.e., $C_s \cdot S_i$ and $C_p \cdot P_j$). The general pattern of autonomic response to the low-intensity stimulus is distributed predominantly along the diagonal of coactivity, whereas that to the high-intensity stimulus lies largely along a line parallel to the sympathetic axis (uncoupled sympathetic mode), with a late occurring parasympathetic withdrawal (reciprocal sympathetic mode).

Although interactions between the autonomic divisions (I_{ij}) have been demonstrated, omission of the interaction term did not seriously confound the observed responses (Figure 4) relative to that predicted from the independent autonomic activities derived from selective blockades. This result may be due in part to the relatively modest basal activational levels, because interactions are most salient at higher levels of sympathetic and parasympathetic activation. Moreover, the cardiac responses entailed relatively small displacements on the autonomic plane and the effector surface (Figure 5). Thus, variance attributable to interactions would be expected to contribute minimally to the observed responses.

The Need for an Autonomic Space Representation

A recent conditioning study illustrates the utility of a representation of cardiac responses in autonomic space and the ambiguity that can result from simple end-organ measures of chronotropic state (Iwata & LeDoux, 1988). Rats were conditioned to an auditory conditioned stimulus (CS) and a shock unconditioned stimulus (US) while cardiovascular measures were obtained. Experimental groups included a forward-conditioning group and a pseudoconditioning group. In spite of the different stimulus contingencies and associative processes in these two groups, both

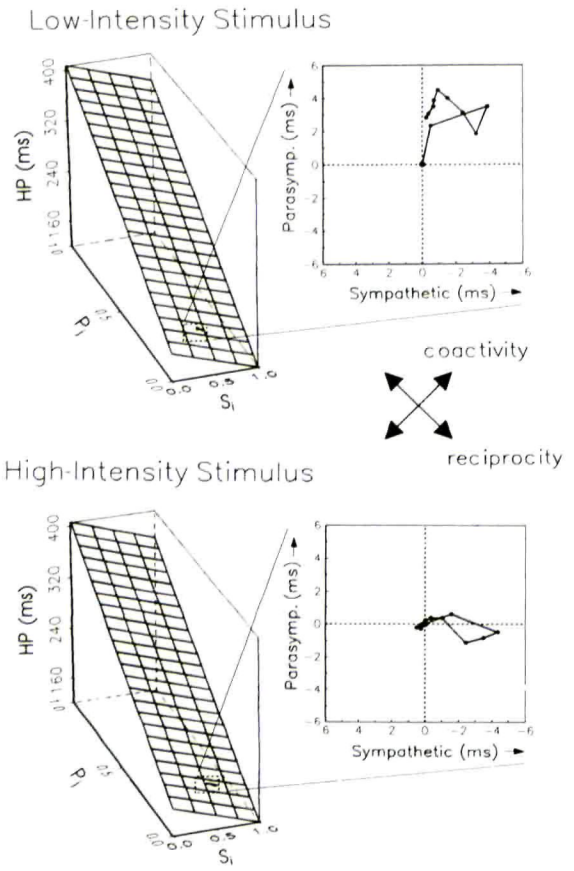

Figure 5. Cardiac responses to a nonsignal acoustic stimulus of two intensities, as depicted on the chronotropic effector surface. The functions depicted on the effector surface are derived from Equation 3 and represent the time-varying loci (2-s intervals) associated with the poststimulus responses depicted in Figure 4. The relevant segments of the effector surface are expanded in the inserts. These inserts depict the cardiac response as movements along the two autonomic axes. For illustration, the axes units of the inserts are expressed in millisecond change in heart period (i.e., $C_s \cdot S_i$ and $C_p \cdot P_j$) from baseline. The large dot at the center (0, 0) of the insert is the basal starting point, and the lines extending from (and returning toward) this basal point depict the temporally unfolding cardiac response. Data points (small dots) depict the cardiac response over 2-s intervals. For clarity, several data points are omitted at the end of the poststimulus time functions. The general pattern of autonomic response to the low-intensity stimulus is distributed predominantly along the diagonal of coactivity, reflecting autonomic coactivation. The data reveal a temporal structure to this coactivation, however, with the initial response (first poststimulus data point) reflecting largely a parasympathetic activation, followed by a sympathetic increment (second poststimulus data point). In contrast, the high-intensity stimulus yielded a response function that lies largely along a line parallel to the sympathetic axis (uncoupled sympathetic mode).

showed a comparable cardioacceleratory response to the CS. Control rats given random presentations of an auditory CS and a shock US uniformly displayed tachycardia in response to the CS, presumably reflecting a nonspecific sensitization. As a group, the forward-paired experimental animals showed a statistically similar mean acceleratory response to the CS. The chronotropic response of the conditioned animals, however, appeared to have an autonomic origin different from that of the response of controls.

Although the overall chronotropic response to the CS was similar for the two groups, pharmacological blockade revealed a fundamental difference in the autonomic bases of these cardiac responses. For the conditioning group, parasympathetic blockade dramatically increased the cardioacceleratory response, suggesting that the CS evoked a concurrent vagal activation that normally dampened the sympathetically driven acceleratory response. Consistent with this interpretation, sympathetic blockade unmasked a notable bradycardia in response to the CS (see Figure 6), which represents the prototypic pattern of coactivation (Berntson et al., 1991). In contrast, the cardioacceleratory response of the pseudoconditioning group was largely eliminated by sympathetic blockade, but this blockade did not unmask a bradycardic response. Moreover, the cardioacceleratory response in this group was largely unaltered by parasympathetic blockade (Figure 6). These results in control animals are consistent with a CS-induced increase in sympathetic drive to the heart (uncoupled sympathetic mode), which may be attributable to nonspecific conditioned fear or anxiety reactions to general contextual cues.

As depicted in the right panels of Figure 6, the predicted response template derived from Equation 3 again showed a relatively good fit with the observed cardiac responses. Although some discrepancy is apparent for the conditioned animals, the unblocked and blockade data were obtained from separate groups of animals, and the discrepancies were within the range of variation seen from group to group in the unblocked condition over three separate experiments.

A representation of these general modes of autonomic response are presented on the effector surface in Figure 7. This figure reveals that the cardiac responses were confined to a relatively small portion of autonomic space, even though they ranged up to 35 bpm change. The expanded displays of Figure 7 reveal a predominant autonomic coactivation in the conditioning group, and a predominant uncoupled sympathetic mode in the pseudoconditioning group. If these results were considered solely from the perspective of the cardiac responses in unblocked animals, no evidence of conditioning would be apparent. Substantive differences between the groups were revealed by selective autonomic blockade, however, which permitted an evaluation of the independent activities of the two autonomic divisions. Vagal blockade revealed a considerably larger sympathetically driven response to the CS in the conditioning group, which was masked in the unblocked conditions by vagal coactivation.

Autonomic Versus Functional Spaces

The autonomic plane and its effector surface offer a general model for characterizing and representing autonomic functions. The baroreceptor–heart rate reflex can be mapped onto the autonomic space model to illustrate two important points. First, as with behavioral variables, even powerful physiological reflexes may occupy only a limited portion of autonomic space. Second, because of transforms imposed by reflex circuits or higher level processes, experimental continua (e.g., blood pressure, stimulus intensity, etc.) may not map linearly onto autonomic axes. For example, a unit change in blood pressure may not uniformly translate into a fixed increment in autonomic outflow. In view of these considerations, we developed an alternative functional space representation that (a) depicts only the relevant subcomponent of autonomic space and (b) offers functional axes units that may be more useful for some types of experimental questions.

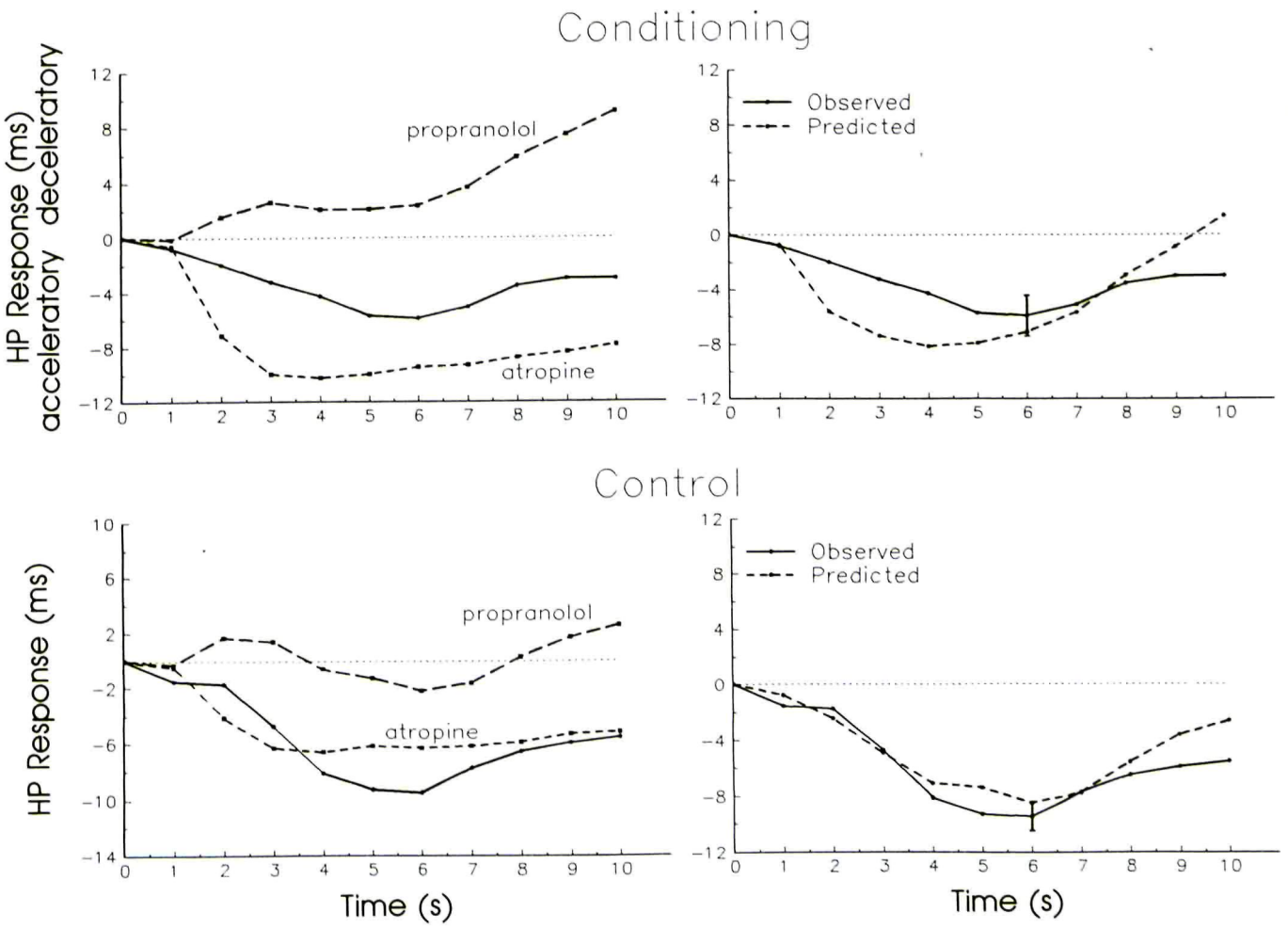

Figure 6. Cardiac responses to an auditory conditioned stimulus (CS) for shock in conditioned and pseudoconditioned animals (*N*s = 8–10). Left panels illustrate responses in the unblocked condition (solid lines) and after sympathetic (propranolol, 1 mg/kg) or parasympathetic (atropine, 2 mg/kg) blockade. Right panels illustrate the observed responses in the unblocked condition and the predicted responses derived from Equation 3. Error bars depict illustrative standard errors for the unblocked response. [Redrawn with permission from Iwata & LeDoux, 1988.]

The Baroreflex: Autonomic Space and the Effector Surface

The data set for baroreflex mapping was derived from the comprehensive study of Head and McCarty (1987). Blood pressure was experimentally manipulated by bolus infusions of the pressor agent phenylephrine and the vasodilator nitroprusside. This study was particularly appropriate because the pressor manipulations were wide enough to cover the entire dynamic range of the baroreflex and because the autonomic bases of the reflex responses were studied by selective pharmacological blockade of the autonomic branches. The general results of this study are illustrated in Figure 8, which displays heart period as a function of blood pressure. The solid line shows the baroreflex relationship in the unblocked condition, and dashed lines indicate the corresponding functions under sympathetic and parasympathetic blockade. The bottom panel of Figure 8 shows the observed baroreflex function and the predicted function derived from Equation 3, based on the independent activities of the autonomic branches under selective blockade. There is close agreement between the observed and predicted functions, even in the absence of an interaction term.

The data obtained under selective autonomic blockades provide the marginal functions needed to map the reflex onto the autonomic plane and its effector surface (Figure 9). The baroreflex entails a predominantly reciprocal mode of autonomic control, with a dynamic range that occupies only a limited portion of autonomic space. Figures 8 and 9 also illustrate the fundamental nonlinearity between blood pressure and both heart period and the autonomic axes. This nonlinearity is most apparent in the asymptotic portions of the baroreflex function, where further blood pressure variations have no appreciable impact on autonomic outflows or heart period. The nonlinearities in the transform of blood pressure onto autonomic axes is illustrated in the insert of Figure 9, which shows the relationship between equal increments (10 mmHg) in blood pressure and units of autonomic activation. The spacing of these blood pressure units is not equivalent along the autonomic axes and necessarily become especially compressed in the asymptotic regions of the baroreflex.

The nonlinear mapping of blood pressure onto the autonomic axes may be partly attributable to the proximity of the lower asymptote to the sympathetic maxima and parasympa-

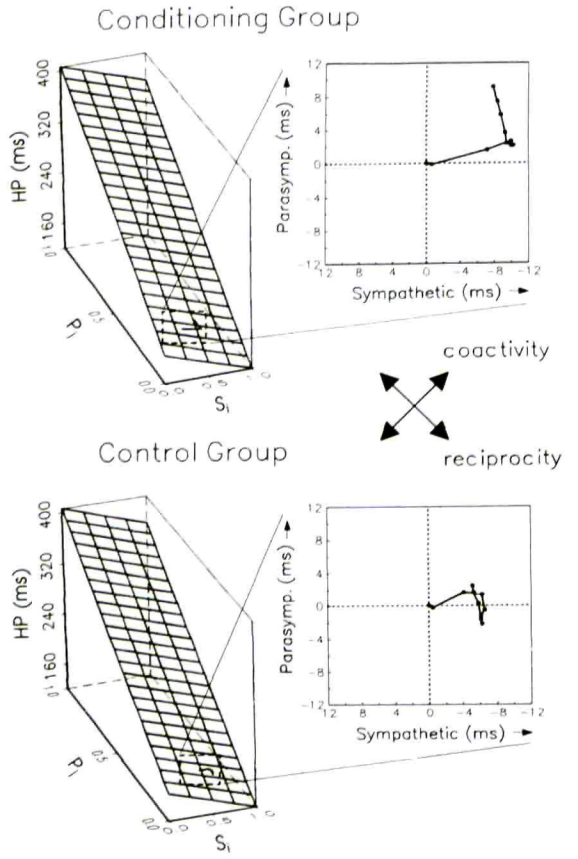

Figure 7. Cardiac responses to an auditory conditioned stimulus in conditioned and pseudoconditioned animals (from Figure 6), as depicted on chronotropic effector surface. The relevant segments of the effector surface are expanded in the inserts, which depict the cardiac response as movements along the two autonomic axes. For illustration, the axes units of the inserts are expressed in millisecond change in heart period (i.e., $C_s \cdot S_i$ and $C_p \cdot P_j$) from baseline. The large dot at the center (0, 0) of the insert is the basal starting point, and the lines extending from this basal point depict the temporally unfolding cardiac response. Data points (small dots) depict the second-by-second cardiac responses. The general pattern of autonomic response in the conditioned animals is distributed predominantly along the diagonal of coactivity. This response revealed a clear temporal structure, with an initial progressive sympathetic activation over the first few seconds followed by parasympathetic activation. The response of pseudoconditioned animals lies predominantly along a line parallel to the sympathetic axis (uncoupled sympathetic mode), although smaller fluctuations in parasympathetic control are also apparent.

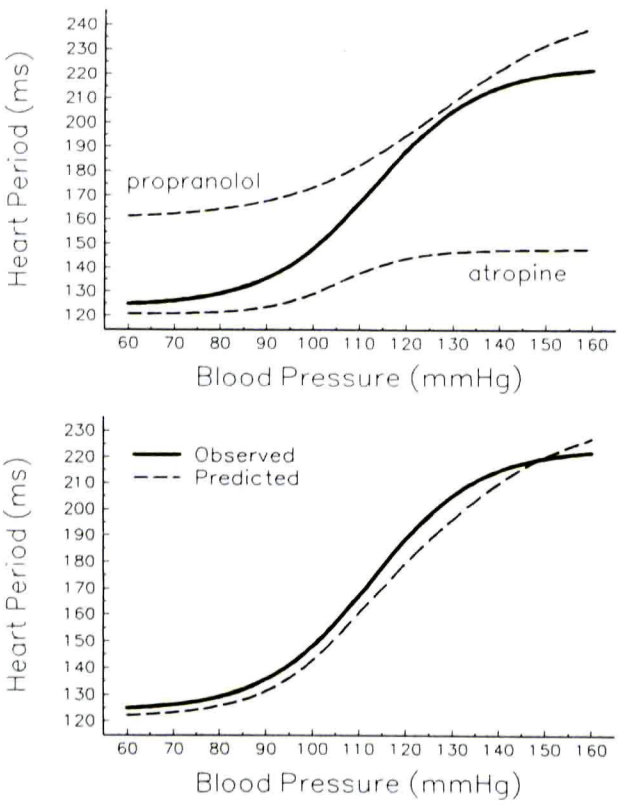

Figure 8. Baroreflex-heart period function. Upper panel illustrates the covariation of heart period with mean arterial pressure in the unblocked control condition (solid function) and after sympathetic (propranolol) or parasympathetic (atropine) blockade. The lower panel illustrates the observed unblocked response and the predicted function derived from Equation 3, based on the independent responses of the autonomic branches under selective blockades. [Redrawn with permission from Head & McCarty, 1987.]

thetic minima of autonomic space (lower right corner of Figure 9). The parallel nonlinearities at the upper asymptote cannot be accounted for by limits of autonomic space, however, because the function does not approach autonomic boundaries at that point. Rather, the nonlinear mapping of the baroreflex onto the autonomic axes appears to arise in part from nonlinearities in the baroreceptors and/or reflex circuits (Spyer, 1990).

The limitations in the range of autonomic control achieved by the baroreflex and the nonlinear mapping of blood pressure onto the autonomic axes suggest an alternative representation of the baroreflex and other functional or psychophysiological relationships. This representation entails a restricted mapping onto a subcomponent of autonomic space and a rescaling of the axes into functional (e.g., physiological, stimulus, or behavioral) units.

The Functional Plane and Its Overlying Surface

Figures 5–9 illustrate that autonomic responses evoked by behavioral or reflexive stimuli may occupy only a limited range of autonomic space. Hence, psychophysiological responses could be represented within a subcomponent of this space, as depicted in the inserts of Figures 5, 7, and 9. Natural boundaries of these autonomic subspaces are the maximal ranges of the autonomic axes over which movements are possible with a given class of stimuli or within a given experimental context.

For psychophysiological studies, it may also be desirable to express the axes of this subspace in functional units corresponding to experimentally relevant independent variables, such as shock intensity, tone frequency, or blood pressure. As for the baroreflex, these functional units may not map linearly onto the autonomic axes. Frequently, the transforms from antecedent stimuli to physiological or behavioral effects assume a sigmoidal shape, with a lower asymptote below threshold and an upper asymptote reflecting ceiling effects, as in the baroreflex functions of Figure 8.

In the full autonomic space maps considered thus far, these nonlinearities are excluded, because these maps were restricted

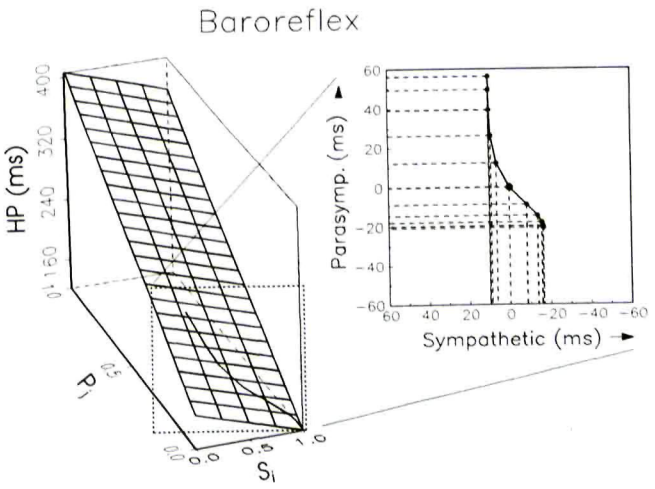

Figure 9. Baroreflex–heart period function (from Figure 8), as depicted on the effector surface. The relevant segment of the underlying autonomic space is expanded in the insert, which depicts the chronotropic states associated with varied blood pressure as displacements along the two autonomic axes. For illustration, the axes units of the inserts are expressed in millisecond change in heart period (i.e., $C_s \cdot S_i$ and $C_p \cdot P_j$) from resting baseline. The large dot at the center (0, 0) of the insert is the basal starting point, and the remaining data points (small dots) depict the chronotropic state for each 10-mmHg change. (Because of the size of the baroreflex response, the axes of the insert extend beyond the boundaries of the effector surface.) The solid line represents the baroreflex function extending from 60 mmHg (lowest data point in the insert) to 160 mmHg (upper data point). The dotted lines extending from the data points to the sympathetic and parasympathetic axes illustrate the nonlinear mapping of the equivalent 10-mmHg steps onto the autonomic axes. The general autonomic mode of the baroreflex is reciprocal, although with progressively increasing blood pressure the baroreflex function is characterized largely by uncoupled parasympathetic activation.

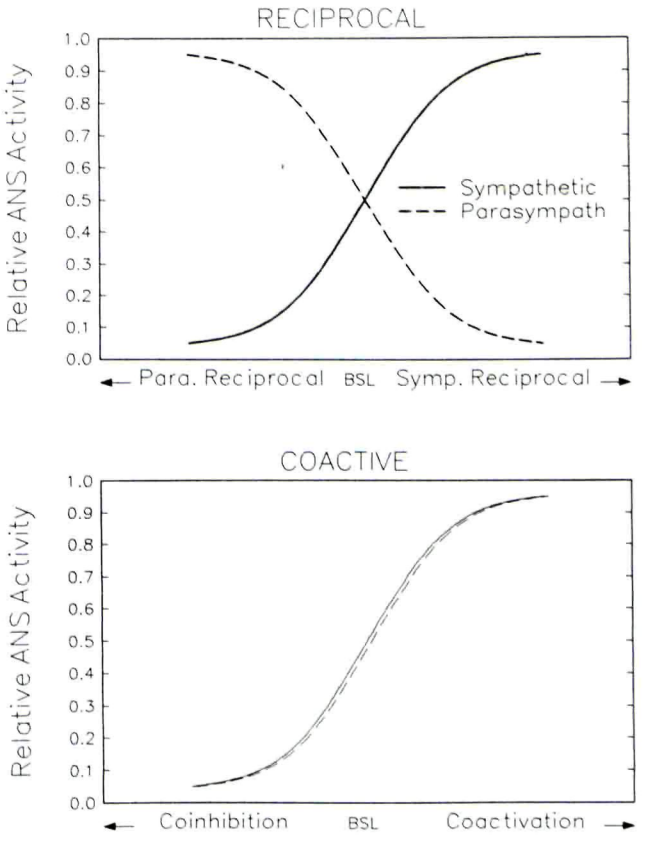

Figure 10. Example sigmoidal antecedent activation functions. The upper panel depicts a reciprocal mode of response of the two autonomic divisions, and the lower panel illustrates a coactive mode. These activation functions represent the changes in the activities of the two autonomic branches (S_i and P_j) as a function of an antecedent activating continuum.

to the relationship between autonomic outflows and cardiac chronotropy. Alternatively, the axes could be expressed in functional units, in which case the resulting surface would reflect the effects of antecedent manipulations on the autonomic control of the target-organ state. That is, the functional surface would capture both the relationship between antecedents and autonomic outflows and the relationship between autonomic outflows and organ effects. In a previous theoretical review, we modeled functional surfaces for a wide variety of sigmoidal antecedent activation functions (Berntson et al., 1991). This modeling revealed common features of functional surfaces that transcend specific shapes or slopes of the activation sigmoids, which may vary from antecedent to antecedent. The alternative perspective offered by these functional surfaces renders some psychophysiological principles and relationships more readily apparent than the full effector surface.

As illustrated in Figure 10, a given antecedent stimulus or condition can be characterized by its sigmoidal activation effects on the two autonomic branches. This antecedent activation may yield coactivation, reciprocal activation, or uncoupled activity of the autonomic branches. The activation functions of Figure 10, together with intermediate forms, yield the functional surface illustrated in Figure 11. With the axes expressed in units of antecedent activation, the functional surface reflects the impact of this antecedent on the functional state of the organ. The antecedent activation sigmoids are apparent in the sympathetic and parasympathetic marginals of the functional surface, where one autonomic division varies and the other remains constant. Reciprocal modes of control lie along or parallel to the left to right diagonal, coactive modes are along or parallel to the front to back diagonal, and uncoupled modes lie parallel to the axes.

Laws of autonomic constraint. The functional surface of Figure 11 illustrates three laws of autonomic constraint, as previously enumerated (Berntson et al., 1991). The law of dynamic range asserts that psychophysiological lability is constrained by the topographic features of the functional surface and its autonomic boundaries. The effect of baseline state on phasic reactivity has long been recognized (Lacey & Lacey, 1962; Wilder, 1931, 1967). An increase in basal heart period from the middle of the functional surface to the maxima at the left axes intersection of Figure 11, for example, would preclude further heart period increases because autonomic boundaries had been reached. This is the essence of the law of initial values (LIV), which asserts a dependency of phasic response on initial baseline levels. The law of dynamic range is broader than the law of initial values, however, and incorporates additional constraints on reactivity to which the LIV is blind. Changes in basal state along the coactive diagonal (front to rear axes intersections

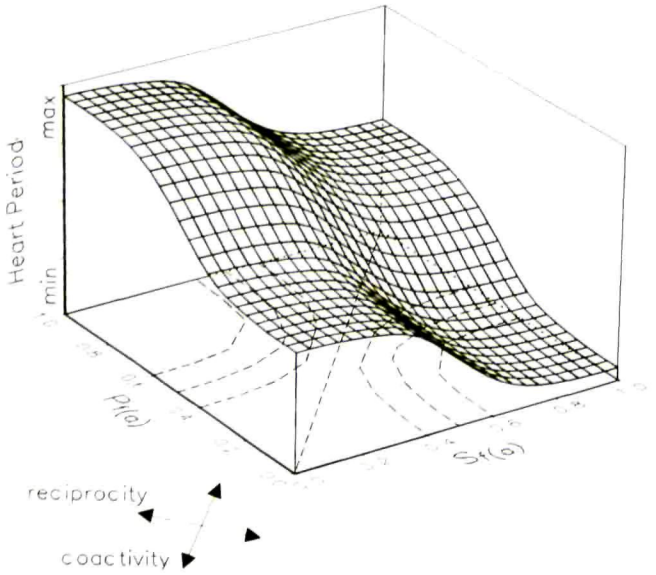

Figure 11. Autonomic functional space and surface. The parasympathetic and sympathetic axes are expressed as functions of antecedent activation conditions ($S_{f(a)}$), rather than as units of autonomic outflow. The sigmoidal functions apparent along the marginals represent the activation functions of Figure 10. The overlying surface depicts the relative chronotropic state of the heart, as derived from Equation 3, for all loci on the functional plane. Dotted lines on the functional space represent isoeffector contour lines, illustrating loci within autonomic space that have equivalent functional effects on the end organ.

of Figure 11) are not associated with alterations in the functional state of the organ, and hence the LIV does not apply. Nevertheless, basal changes along this diagonal are associated with dramatically different autonomic constraints. For a baseline locus at the rear axes intersection, no further sympathetic or vagal activation is possible. A baseline locus at the front axes intersection, however, although associated with the same basal heart period, would not preclude either sympathetic or vagal activation. Rather, modes of sympathetic or vagal withdrawal would now be precluded. Because the constraints on autonomic reactivity along the coactivity dimension are not associated with notable variations in the tonic state of the organ, the broader set of autonomic constraints cannot be derived from baseline measures alone.

In addition to the limits of dynamic range, constraints on organ lability are imposed by the direction of movement within autonomic space. The law of reactive lability maintains that a unit movement, from a given locus in autonomic space, yields varying magnitudes of organ response as a function of the mode of autonomic control. A given movement along the reciprocal diagonal yields a large change in the functional state of the target organ, whereas an equivalent movement along the coactivity diagonal is associated with minimal effects on organ state. The essence of the law of reactive lability is that constraints on target organ lability, associated with the modes of autonomic control, are apparent even at loci remote from dynamic range boundaries.

The law of directional stability asserts that there are fundamental differences in the directional consistency of target organ response associated with different modes of autonomic control. For reciprocal responses, such as sympathetic activation and parasympathetic withdrawal, the changes in each autonomic branch yield synergistic responses in the target organ. Hence, variations in the relative changes of the two divisions do not alter the direction of the target organ response. In contrast, coactive modes entail conjoint activation of the autonomic divisions, which yield opposite organ responses. Consequently, the direction of target organ response is highly dependent on the relative dominance of the sympathetic or parasympathetic responses. Movements directly along the coactivity diagonal may yield no organ response, whereas parallel movement vectors on opposite sides of the coactivity diagonal yield organ responses of opposite direction.

The laws of autonomic constraint impose fundamental limitations on visceral responses. In some cases, these constraints are intuitive, such as for the law of dynamic range. In other instances, constraints are less obvious. The law of directional stability, for example, asserts that a specific movement within autonomic space can yield diametrically opposite organ responses, depending on the locus from which the movement begins. Moreover, the law of reactive lability further qualifies the magnitude of this organ response, depending on the specific direction of movement from a given basal point. Although not intuitively obvious, the functional surface representation of Figure 11 permits a spatial visualization of these relationships.

The baroreflex and its functional surface. The discussion above illustrates some general features of autonomic functional surfaces. In the present section, we illustrate the mapping of the baroreflex onto an empirically instantiated functional surface. Because the level of sympathetic and parasympathetic activation is directly related to blood pressure (see Figure 8), the autonomic axes (S_i and P_j) of Equation 3 could be expressed as functions of mean arterial pressure: $S_i = f_s(MAP)$ and $P_j = f_p(MAP)$.

Figure 12 illustrates the baroreflex plane and associated functional surface, with axes specified in linear units of mean arterial pressure (mmHg), and with the axes bounded by the dynamic range of the baroreflex. The sigmoidal functions relating blood pressure to activities in the two autonomic branches are apparent at the sympathetic and parasympathetic marginals. The nonlinearities of this surface reflect the fact that, in addition to the linear transform between autonomic outflows and organ effects, the functional surface also incorporates the nonlinear transform from antecedent stimuli (blood pressure in this case) to autonomic outflows.

The functional surface of Figure 12 offers a graphical depiction of the nonlinearities inherent in the transform from the antecedent condition (blood pressure) to the chronotropic state of the heart. In the baroreflex example, the functional surface represents merely a conceptual model for illustration. This surface could not be fully realized empirically because the units of the functional axes (mmHg) are equivalent, so that translation along one axis is necessarily associated with an equivalent translation along the other. Given variations in blood pressure, the empirical function would lie along a single vector on the autonomic surface (see Figure 12). With orthogonal axes units related to distinct antecedents, however, the full functional surface could be manifest empirically. Given the essential linearity between autonomic outflows and heart period, the functional surface would represent a topological model of the nonlinearities inherent in the transformation from antecedent conditions to autonomic outflows. This functional surface depiction affords an important perceptual representation of the modes of

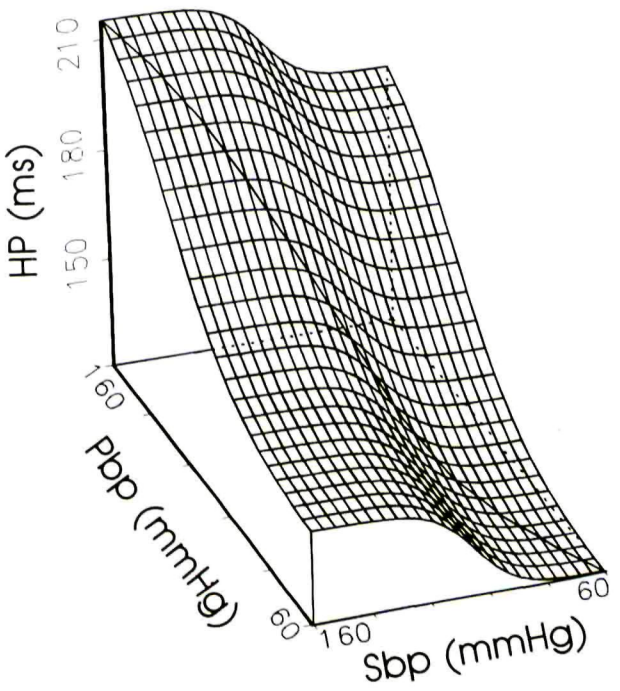

Figure 12. Baroreflex functional space and surface. The parasympathetic and sympathetic axes are expressed in functional units of blood pressure. The sigmoidal functions apparent along the marginals represent the independent activities of the autonomic branches (from Figure 8), as obtained under selective autonomic blockades. The overlying surface depicts the relative chronotropic state of the heart, as derived from Equation 3, associated with all loci in the functional space. The solid line extending from the lower right to the upper left corner of the functional surface illustrates the baroreflex–heart period function of Figure 8.

autonomic control and the target-organ impact of psychophysiological antecedents.

Summary of effector versus functional surfaces. The effector and functional surfaces of Figures 9 and 12 do not represent mutually exclusive alternatives. Psychophysiological relationships entail two major classes of transforms: from psychophysiological antecedents to central autonomic outflows and from autonomic outflows to functional effects on end organs. The full autonomic plane and effector surface capture the second of these transformations, whereas the functional space and surface incorporate both, albeit within a restricted area of the full effector surface. The functional and full effector surfaces offer complementary perspectives, because they differentially emphasize or illuminate specific psychophysiological relationships. The discussion of functional surfaces is limited here to the illustration of the relationship between psychophysiological antecedents and autonomic space. We will further develop the concept and representation of functional surfaces in a subsequent paper.

Interactions Between the Autonomic Divisions

The effector surfaces in Figures 5, 7, and 9 are based on a simple additive model of the independent activities of the autonomic branches. Potential interactions among the branches in the unblocked condition could alter the shapes of these surfaces. Although the autonomic branches exert opposing actions on the sinoatrial node, the net autonomic effect on cardiac chronotropy is not always a simple algebraic sum of the independent actions of the two divisions. Rather, inhibitory interactions among the autonomic branches are known to exist in both directions (Hall & Potter, 1990; Levy, 1984; Levy & Zieske, 1969; Manabe et al., 1991; Warner & Levy, 1989; Yang & Levy, 1984). The most powerful and well established of these is a vagal inhibition of sympathetic chronotropic effects. Although in some laboratory conditions high levels of vagal activity may completely obscure sympathetic effects on the heart, the magnitude of interaction under normal physiological conditions is less clear. This issue is further clouded by the fact that high levels of sympathetic activity can also inhibit parasympathetic control through the release of neuromodulators (e.g., neuropeptide Y), which are colocalized in sympathetic terminals (Hall & Potter, 1990; Levy, 1984; Manabe et al., 1991). These neuromodulators have a relatively long latency and time course, which would minimize their appearance in acute nerve stimulation studies. Further complexities arise because interactions among autonomic nerves are strikingly dependent on the phase relationships between the vagal and sympathetic activities (Yang & Levy, 1984).

Based on conjoint nerve stimulation studies in anesthetized preparations, Levy and Zieske (1969) reported an approximately 60% reduction in sympathetic chronotropic effects with vagal stimulation in the dog, and Smith (1972) reported an approximately 50% inhibition in the rabbit. A recent study has examined autonomic interactions under more natural conditions, with sympathetic activation induced by exercise in unanesthetized free-moving dogs (Stramba-Badiale et al., 1991). Under these conditions, vagal stimulation through chronically implanted electrodes yielded a maximum inhibition of exercise-induced tachycardia of approximately 25%.

Although interactions among the autonomic branches do not alter representations of psychophysiological responses on the autonomic plane, they can distort the cardiac effector surface. These interactions would be expected to be maximal at high levels of vagal and sympathetic activity. Indeed, no interactions would be possible at three of the four corners of autonomic space, where activity of one or both of the autonomic divisions is null. Hence, potential interactions would not confound the estimate of HPp_{max} (left axis intersection), HPs_{max} (right axis intersection), or β (front axis intersection). Potential interactions would be greatest at the rear axis intersection, where sympathetic and parasympathetic activities are maximal, and would be expected to decline as a function of distance from this point.

Although interactions among the autonomic branches certainly warrants additional study, the existence of such interactions would not seriously distort the analysis presented here. Figure 13 shows the expected effect on the effector surface of a 50% vagal inhibition of sympathetic chronotropic control at maximal levels of activation. This effect would cant the rear corner of the surface upward along the z-axis by 21 ms, elevating it half-way toward the parasympathetic maximum. The effect of the interaction would be expected to decrease as one moved away from the rear axes intersection. A linear decline is modeled in Figure 13. At basal autonomic levels in the rat (from Figures 5, 6, and 7), this decline would translate into a discrepancy of less than 1% ($\approx$1.5 ms) in the estimate of basal heart period derived from Equation 3. Moreover, given the largest heart period response reported by Iwata and LeDoux (1988) in a con-

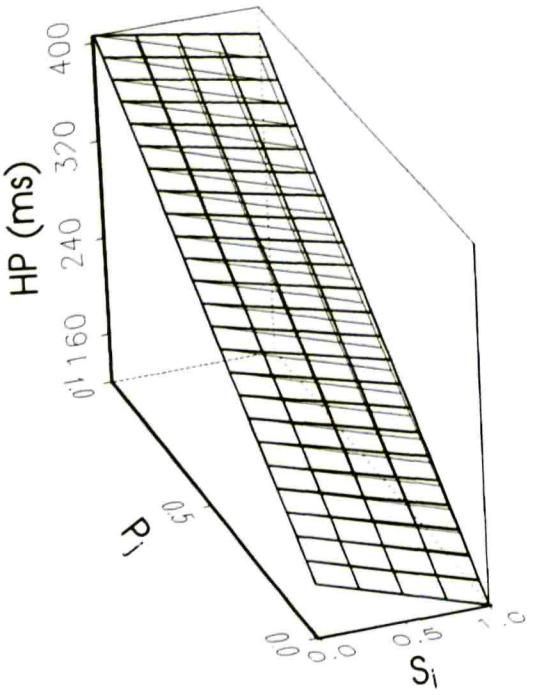

Figure 13. Effect of interactions among the autonomic branches on the effector surface. The upper surface depicts the consequences of vagal inhibition of sympathetic chronotropic effects. The lower surface illustrates the effector surface in the absence of interactions. The upper surface is modeled on a 50% inhibition of sympathetic chronotropic effects at maximal vagal activity.

ditioned aversion paradigm (≈9 ms or 35 bpm; see Figure 7), this interaction would distort the expected response amplitude by approximately 0.8 ms, or less than 9%.

The minimal impact of interactions is also indicated by the generally close agreement between observed cardiac responses and predicted functions based on the independent activities of the sympathetic and parasympathetic divisions in the absence of an interaction term. Indeed, the baroreflex manipulation resulted in the largest displacement on autonomic space and would be expected to involve the largest bias from autonomic interactions. Potential interactions would yield a discrepancy between the observed baroreflex function in the unblocked condition and the function predicted from Equation 3 (with the interaction term set to 0). In fact, there was a close correspondence between the predicted and observed functions (see Figure 8). The relatively small interaction effect may be attributable to several factors, including (a) the limited range of psychophysiological responses, relative to the full autonomic space, (b) the fact that basal locations in autonomic space are close to the front axes intersection, where the effects of interactions would be minimal, and (c) the reciprocal mode of response, which precludes high concurrent levels of activity in both autonomic branches.

We do not suggest that interactions are trivial. The quantitative enumeration of autonomic interactions would only further increase the theoretical and practical significance of the proposed model of autonomic space. Rather, for the initial development of an autonomic space model, the absence of an interaction term is unlikely to seriously distort interpretations of psychophysiological responses in most behavioral paradigms.

Extension of the Autonomic Space Model to Humans

The model of autonomic space as developed here has considerable implications for psychophysiological theory and measurement. Although the principles derived from the present analysis apply even in the absence of an explicit model of autonomic space in humans, the development of such a model clearly would be desirable. This development should be relatively straightforward, and much of the requisite information is extant in the current literature.

Direct stimulation studies of cardiac nerves indicate that humans, like other animals, have a relatively linear autonomic space up to asymptotic levels (Carlson et al., 1992; Carlsten et al., 1957). Maximal baroreflex activation and exercise could provide an estimate of HPs_{max} and have been extensively documented in human studies, including the requisite studies of autonomic blockade (Ekblom et al., 1973; Jose, Stitt, & Collison, 1970; Lewis, Nylander, Gad, & Areskog, 1980; Ribeiro, Ibanez, & Stein, 1991; Robinson, Epstein, Beiser, & Braunwald, 1966; Rowell, 1986). Similarly, HPp_{max} can be estimated from potent vagal reflexes and from the maximal heart period under vagal stimulation (Carlson et al., 1992). Intrinsic heart period can be determined from effects of dual pharmacological blockade of the autonomic branches (Lewis et al., 1980; Ribeiro et al., 1991; Robinson et al., 1966; Sutton, Cole, Gunning, Hickie, & Seldon, 1967). Additional information on the intrinsic rate may be available from denervated transplanted hearts (McLaughlin et al., 1978; Pope, Stinson, Daughters, Ingels, & Alderman, 1980; Sloan et al., 1990). Although the specific parameters of autonomic space for the human will differ from those of the rat, general features of autonomic space and the effector surface may be highly similar. For example, chronotropic control appears to be linearly related to neural activity in both rats and humans, and the vagal nerve has a considerably wider dynamic range than does the sympathetic division in both species.

An important consideration that arises in the development of a model of autonomic space for the human is the likely differences in the parameters of the equation across age, sex, state of aerobic conditioning, or other individual differences. Although such factors can readily be controlled in animal work, human studies may be more limited in their ability to assess or control for these factors. Hence, autonomic space models may be restricted in the subject populations to which they can be applied. This issue should be investigated further, but these variables may be less problematic than they might appear. Although β in humans varies with age and aerobic conditioning, these relationships are lawful and specifiable (Jose et al., 1970; Lewis et al., 1980; Sutton et al., 1967).

In summary, extension of the autonomic space model to human subjects appears feasible. Much of the basic information necessary for this extension already exists in the psychophysiological and physiological literature. Even in the absence of the quantitative construction of the full autonomic space, analyses can still be applied to more restricted functional spaces. Moreover, the principles derived above are generally applicable to psychophysiological studies.

Conclusions

It will ultimately be important to extend the autonomic space model to humans, as psychophysiological relationships continue to be refined. This imperative is underscored by the early report

of Obrist et al. (1965) that autonomic coactivation is evoked by a conditioned aversive stimulus in human subjects. This observation is consistent with that of Iwata and LeDoux (1988) in the rat and underscores the need for a two-dimensional model of autonomic space. Because of the conjoint activation of opposing branches of the ANS, coactive modes of autonomic control yield a fundamentally unstable directional response in target organs (Berntson et al., 1991). Depending on which division dominates, the cardiac response may be either tachycardia or bradycardia. Consequently, the inherent order in psychophysiological relationships may not be apparent when only simple measures of end-organ state are obtained. Rather, the modes of autonomic control may have a more consistent relationship with psychological variables. Thus, the human subjects in the Obrist et al. (1965) study displayed bradycardia to the conditioned aversive stimulus, whereas rats in the Iwata and LeDoux (1988) study showed tachycardia. In both cases, however, subjects demonstrated a consistent coactive mode of autonomic control in the aversive conditioning context.

The importance of the two-dimensional model of autonomic space does not lie merely in its ability to more accurately depict psychophysiological responses. Rather, this model offers a conceptual platform to clarify psychophysiological laws or principles. Although the law of initial values was enumerated over six decades ago (Wilder, 1931, 1967), its fundamental basis and theoretical status have yet to be fully clarified. We have argued elsewhere (Berntson et al., 1991) that the law of initial values can be subsumed by more comprehensive laws of autonomic constraint derived from the autonomic space model. This analysis reveals a number of constraints on autonomic reactivity, only a subset of which are subject to the law of initial values. Movements within autonomic space along isoeffector contours are associated with changing autonomic constraints. Because these movements are not mirrored by alterations in the basal chronotropic state of the heart, those varying constraints are invisible to the law of initial values. These constraints, however, are inherent to the law of dynamic range and to the autonomic space model from which it was derived.

The growing recognition of the need for a more comprehensive characterization of autonomic control is apparent in the increasing efforts to identify components of autonomic activation (Allen & Crowell, 1989; Allen, Obrist, Sherwood, & Crowell, 1987; Johnson & Anderson, 1990; Obrist, 1981; Pollak & Obrist, 1988; Stemmler et al., 1991), and to develop selective noninvasive psychophysiological indices of the autonomic divisions. Among the more promising developments are those in impedance cardiography (Kelsey & Guethlein, 1990; Sherwood, Dolan, & Light, 1990), and efforts to parse frequency components of autonomic response (Berntson, Cacioppo, & Quigley, 1993; Grossman & Wientjes, 1986; Porges, 1986; Porges & Bohrer, 1990). Further developments in these and other areas will likely facilitate the noninvasive measurement of autonomic space.

In summary, a single-vector model of an autonomic continuum leads to an overly restrictive conception of autonomic control, which is belied by established empirical findings. A major obstacle to specifying psychological events as a function of physiological processes [$\psi = f(\phi)$] is the many-to-one mappings that may obtain between autonomic space and organ response and between behavioral variables and autonomic space (Cacioppo & Tassinary, 1990). The present model provides a conceptual platform for the quantitative investigation of these components of psychophysiological relationships and for the selection of appropriate response metrics (i.e., heart period). Representations of autonomic responses in the terms of their fundamental origins would constitute a significant advance in psychophysiology.

REFERENCES

Allen, M. T., & Crowell, M. D. (1989). Patterns of autonomic response during laboratory stressors. *Psychophysiology, 26*, 603–614.

Allen, M. T., Obrist, P. A., Sherwood, A., & Crowell, M. D. (1987). Evaluation of myocardial and peripheral vascular responses during reaction time, mental arithmetic, and cold pressor tasks. *Psychophysiology, 24*, 648–656.

Berger, R. D., Saul, P. S., & Cohen, R. J. (1989). Transfer function analysis of autonomic regulation. I. Canine atrial rate response. *American Journal of Physiology, 256*, H142–H152.

Berntson, G. G., Cacioppo, J. T., & Quigley, K. S. (1991). Autonomic determinism: The modes of autonomic control, the doctrine of autonomic space, and the laws of autonomic constraint. *Psychological Review, 98*, 459–487.

Berntson, G. G., Cacioppo, J. T., & Quigley, K. S. (1993). Respiratory sinus arrhythmia: Autonomic origins, physiological mechanisms, and psychophysiological implications. *Psychophysiology, 30*, 183–196.

Berntson, G. G., Quigley, K. S., Fabro, V. T., & Cacioppo, J. T. (1992). Vagal stimulation and cardiac chronotropy in rats. *Journal of the Autonomic Nervous System, 41*, 221–226.

Bolter, C. P., & Atkinson, K. J. (1988a). Maximum heart rate responses to exercise and isoproterenol in the trained rat. *American Journal of Physiology, 254*, R834–R839.

Bolter, C. P., & Atkinson, K. J. (1988b). Influence of temperature and adrenergic stimulation on rat sinoatrial frequency. *American Journal of Physiology, 254*, R840–R844.

Bolter, C. P., Banister, E. W., & Singh, A. K. (1986). Intrinsic rate and adrenergic responses of atria from rats on sprinting, endurance, and walking exercise programmes. *Australian Journal of Experimental Biology and Medicine, 64*, 251–256.

Cacioppo, J. C., & Tassinary, L. G. (1990). Inferring psychological significance from physiological signals. *American Psychologist, 45*, 16–28.

Cannon, W. B. (1939). *The wisdom of the body*. New York: W. W. Norton.

Carlson, M. D., Geha, A. S., Hsu, J., Martin, P. J., Levy, M., Jacobs, G., & Waldo, A. L. (1992). Selective stimulation of parasympathetic nerve fibers to the human sinoatrial node. *Circulation, 85*, 1311–1317.

Carlsten, A., Folkow, B., & Hamberger, C. A. (1957). Cardiovascular effects of direct vagal stimulation in man. *Acta Physiologica Scandinavica, 41*, 68–76.

Corre, K. A., Cho, H., & Barnard, R. J. (1976). Maximum exercise heart rate reduction with maturation in the rat. *Journal of Applied Physiology, 40*, 741–744.

Daly, M. de B. (1984). Breath-hold diving: Mechanisms of cardiovascular adjustments in the mammal. In P. F. Baker (Ed.), *Recent advances in physiology* (pp. 201–245). Edinburgh: Churchill Livingston.

Dexter, F., Levy, M. N., & Rudy, Y. (1989). Mathematical model of the changes in heart rate elicited by vagal stimulation. *Circulation Research, 65*, 1330–1339.

Ekblom, B., Kilbom, A., & Soltysiak, J. (1973). Physical training, bradycardia, and autonomic nervous system. *Scandinavian Journal of Clinical and Laboratory Investigation, 32*, 251–256.

Ford, T. W., & McWilliam, P. N. (1986). The effects of electrical stimulation of myelinated and non-myelinated vagal fibers on heart rate in the rabbit. *Journal of Physiology, 380*, 341–347.

Fukuda, Y., Sato, A., Suzuki, A., & Trzebski, A. (1989). Autonomic nerve and cardiovascular responses to changing blood oxygen and carbon dioxide levels in the rat. *Journal of the Autonomic Nervous System, 28*, 61–74.

Furukawa, Y., Wallick, D. W., Carlson, M. D., & Martin, P. J. (1990). Cardiac electrical responses to vagal stimulation of fibers to discrete cardiac regions. *American Journal of Physiology, 258*, H1112–H1118.

Gellhorn, E., Cortell, R., & Feldman, J. (1941). The effect of emotion, sham rage and hypothalamic stimulation on the vago-insulin response. *American Journal of Physiology, 132*, 532-541.

Grossman, P., & Wientjes, C. (1986). Respiratory sinus arrhythmias and parasympathetic cardiac control: Some basic issues concerning quantification, application and implications. In P. Grossman, K. H. Janssen, & D. Vaitl (Eds.), *Cardiorespiratory and cardiosomatic psychophysiology* (pp. 117-138). New York: Plenum.

Hall, G. T., & Potter, E. K. (1990). Attenuation of vagal action following sympathetic stimulation is modulated by prejunctional α_2-adrenoceptors in the dog. *Journal of the Autonomic Nervous System, 30*, 129-138.

Head, G. A., & McCarty, R. (1987). Vagal and sympathetic components of the heart rate range and gain of the baroreceptor-heart rate reflex in conscious rats. *Journal of the Autonomic Nervous System, 21*, 203-213.

Huang, T. F., & Peng, Y. I. (1976). Role of the chemoreceptor in diving bradycardia in rat. *Japanese Journal of Physiology, 26*, 395-401.

Iwata, J., & LeDoux, J. E. (1988). Dissociation of associative and nonassociative concomitants of classical fear conditioning in the freely behaving rat. *Behavioral Neuroscience, 102*, 66-76.

Johnson, A. K., & Anderson, E. A. (1990). Stress and arousal. In J. T. Cacioppo & L. G. Tassinary (Eds.), *Principles of psychophysiology: Physical, social and inferential elements* (pp. 216-252). New York: Cambridge University Press.

Jose, A. D., Stitt, F., & Collison, D. (1970). The effects of exercise and changes in body temperature on the intrinsic heart rate in man. *American Heart Journal, 79*, 488-498.

Katona, P. G., Poitras, G., Barnett, O., & Terry, B. S. (1970). Cardiac vagal efferent activity and heart period in the carotid sinus reflex. *American Journal of Physiology, 218*, 1030-1037.

Kelsey, R. M., & Guethlein, W. (1990). An evaluation of the ensemble averaged impedance cardiogram. *Psychophysiology, 27*, 1-23.

Kerin, N. Z., Louridas, G., Edelstein, J., & Levy, M. N. (1983). Interactions among the critical factors affecting sinus node function: The quantitative effects of the duration and frequency of atrial pacing and of vagal and sympathetic stimulation upon overdrive suppression of the sinus node. *American Heart Journal, 105*, 215-223.

Koizumi, K., Kollai, M., & Terui, N. (1986). The physiology of cardiac innervation: Relationships between cardiac vagal and sympathetic nerve activities. *Journal of the Autonomic Nervous System, 13*(Suppl.), 161-171.

Koizumi, K., Terui, N., & Kollai, M. (1983). Neural control of the heart: Significance of double innervation re-examined. *Journal of the Autonomic Nervous System, 7*, 279-294.

Koizumi, K., Terui, N., & Kollai, M. (1985). Effect of cardiac vagal and sympathetic nerve activity on heart rate in rhythmical fluctuation. *Journal of the Autonomic Nervous System, 12*, 251-259.

Lacey, J. I., & Lacey, B. C. (1962). The law of initial values in the longitudinal study of autonomic constitution: Reproducibility of autonomic response patterns over a four year interval. *Annals of the New York Academy of Sciences, 98*, 1257-1290.

Levy, M. N. (1984). Cardiac sympathetic-parasympathetic interactions. *Federation Proceedings, 43*, 2598-2602.

Levy, M. N., & Zieske, H. (1969). Autonomic control of cardiac pacemaker activity and atrioventricular transmission. *Journal of Applied Physiology, 27*, 465-470.

Lewis, S. F., Nylander, E., Gad, P., & Areskog, N.-H. (1980). Non-autonomic component in bradycardia of endurance trained men at rest and during exercise. *Acta Physiologica Scandinavica, 109*, 297-305.

Lin, Y. C. (1974). Autonomic nervous control of cardiovascular response during diving in the rat. *American Journal of Physiology, 227*, 601-604.

Lin, Y. C., & Horvath, S. M. (1972). Autonomic control of cardiac frequency in the exercise trained rat. *Journal of Applied Physiology, 33*, 796-799.

Manabe, N., Foldes, F. F., Töröcsik, A., Nagashima, H., Goldiner, P. L., & Vizi, E. S. (1991). Presynaptic interaction between vagal and sympathetic innervation in the heart: Modulation of acetylcholine and noradrenaline release. *Journal of the Autonomic Nervous System, 32*, 233-242.

McLaughlin, P. R., Kleiman, J. H., Martin, R. P., Doherty, P. W., Reitz, B., Stinson, E. B., Daughters, G. T., Ingels, N. B., & Alderman, E. L. (1978). The effect of exercise and atrial pacing on left ventricular volume and contractility in patients with innervated and denervated hearts. *Circulation, 58*, 476-483.

Murphy, C. A., Sloan, R. P., & Myers, M. M. (1991). Pharmacologic responses and spectral analyses of spontaneous fluctuations in heart rate and blood pressure in SHR rats. *Journal of the Autonomic Nervous System, 36*, 237-250.

Obrist, P. A. (1981). *Cardiovascular psychophysiology*. New York: Plenum.

Obrist, P. A., Wood, D. M., & Perez-Reyes, M. (1965). Heart rate during conditioning in humans: Effects of UCS intensity, vagal blockade, and adrenergic block of vasomotor activity. *Journal of Experimental Psychology, 70*, 32-42.

Parker, P., Celler, B. G., Potter, E. K., & McCloskey, D. I. (1984). Vagal stimulation and cardiac slowing. *Journal of the Autonomic Nervous System, 11*, 226-231.

Pollak, M. H., & Obrist, P. A. (1988). Effects of autonomic blockade on heart rate responses to reaction time and sustained handgrip tasks. *Psychophysiology, 25*, 689-695.

Pope, S. E., Stinson, E. B., Daughters, G. T., Ingels, N. B., & Alderman, E. L. (1980). Exercise response of the denervated heart in long-term cardiac transplant recipients. *American Journal of Cardiology, 46*, 213-218.

Porges, S. W. (1986). Respiratory sinus arrhythmia: Physiological basis, quantitative methods, and clinical implications. In P. Grossman, K. Janssen, & D. Vaitl (Eds.), *Cardiorespiratory and cardiosomatic psychophysiology* (pp. 101-115). New York: Plenum.

Porges, S. W., & Bohrer, R. E. (1990). Analyses of periodic processes in psychophysiological research. In J. T. Cacioppo & L. G. Tassinary (Eds.), *Principles of psychophysiology: Physical, social and inferential elements* (pp. 708-753). New York: Cambridge University Press.

Quigley, K. S., & Berntson, G. G. (1990). Autonomic origins of cardiac responses to nonsignal stimuli in the rat. *Behavioral Neuroscience, 104*, 751-762.

Randall, D. C., Kaye, M. P., Randall, W. C., Brady, J. V., & Martin, K. H. (1976). Response of primate heart to emotional stress before and after cardiac denervation. *American Journal of Physiology, 230*, 988-995.

Randall, W. C., Kaye, M. P., Thomas, J. X., & Barber, B. A. (1980). Intrapericardial denervation of the heart. *Journal of Surgical Research, 29*, 101-109.

Ribeiro, J. P., Ibanez, J. M., & Stein, R. (1991). Autonomic nervous control of the heart rate response to dynamic incremental exercise: Evaluation of the Rosenbleuth-Simeone model. *Journal of Applied Physiology, 62*, 140-144.

Robinson, B. F., Epstein, S. E., Beiser, G. D., & Braunwald, E. (1966). Control of heart rate by the autonomic nervous system. *Circulation Research, 14*, 400-411.

Rosenbleuth, A. (1932). The chemical mediation of autonomic nervous impulses as evidenced by summation of responses. *American Journal of Physiology, 102*, 12-38.

Rowell, L. B. (1986). *Human circulation regulation during physical stress*. New York: Oxford University Press.

Sherrington, C. S. (1906). *The integrative action of the nervous system*. New Haven, CT: Yale University Press.

Sherwood, A., Dolan, C. A., & Light, K. C. (1990). Hemodynamics of blood pressure response during active and passive coping. *Psychophysiology, 27*, 656-668.

Sloan, R. P., Shapiro, P. A., & Gorman, J. M. (1990). Psychophysiological reactivity in cardiac transplant recipients. *Psychophysiology, 27*, 187-194.

Smith, D. C. (1972). Heart rate effects of combined vagal and stellate stimulation in atropinized rabbits. *American Journal of Physiology, 222*, 546-549.

Sonne, B., & Galbo, H. (1980). Simultaneous determinations of metabolic and hormonal responses, heart rate, temperature and oxygen uptake in running rats. *Acta Physiologica Scandinavica, 109*, 201-209.

Spyer, K. M. (1990). The central nervous organization of reflex circulatory control. In A. D. Loewy & K. M. Spyer (Eds.), *Central regulation of autonomic function* (pp. 1168-1188). New York: Oxford University Press.

Stemmler, G., Grossman, P., Schmid, H., & Foerster, F. (1991). Towards a systematization of laboratory tasks in cardiovascular research: A model of cardiovascular activation components for stud-

ies using autonomic receptor antagonists. *Psychophysiology, 28,* 367–382.

Stramba-Badiale, M., Vanoli, E., De Ferrari, G. M., Cerati, D., Foreman, R. D., & Schwartz, P. J. (1991). Sympathetic-parasympathetic interaction and accentuated antagonism in conscious dogs. *American Journal of Physiology, 260,* H335–H340.

Sutton, J. R., Cole, A., Gunning, J., Hickie, J. B., & Seldon, W. A. (1967). Control of heart-rate in healthy young men. *Lancet, 2,* 1398–1400.

Tucker, D. C., & Domino, J. V. (1988). Balance among autonomic controls of heart rate in neonatal spontaneously hypertensive and borderline hypertensive rats. *Journal of the Autonomic Nervous System, 22,* 11–21.

Versprille, A., & Wise, M. E. (1971). Quantitative effect of vagal stimulation on heart interval in newborn and older rabbits. *Pflügers Archives, 325,* 61–76.

Warner, M. R., & Levy, M. N. (1989). Neuropeptide Y as a putative modulator of the vagal effects on heart rate. *Circulation Research, 64,* 882–889.

Wilder, J. (1931). The "Law of Initial Values," a neglected biological law and its significance for research and practice. In S. W. Porges & M. G. H. Coles (Eds.), *Psychophysiology* (pp. 47–55). Stroudsberg, PA: Dowden, Hutchinson & Ross.

Wilder, J. (1967). *Stimulus and response: The law of initial value.* Bristol: J. Wright.

Yang, T., & Levy, M. N. (1984). The phase-dependency of the cardiac chronotropic responses to vagal stimulation as a factor in sympathetic-vagal interactions. *Circulation Research, 54,* 703–710.

(Received July 28, 1992; Accepted March 10, 1993)